

1 Coexistence of alleles: insights of Modern
2 Coexistence Theory into the maintenance of
3 genetic diversity

4 Alba Cervantes-Loreto¹, Michelle L. Marraffini¹, Daniel B. Stouffer¹, and
5 Sarah P. Flanagan¹

6 ¹Centre for Integrative Ecology, School of Biological Sciences, University of Canterbury,
7 Christchurch 8140, New Zealand

Words in abstract	to be determined
Words in manuscript	to be determined
Number of references	to be determined
Number of figures	to be determined
Number of tables	2
Number of text boxes	0
Corresponding author	Alba Cervantes-Loreto
Phone	+64 369 2880
Email	alba.cervantesloreto@pg.canterbury.ac.nz

1 Introduction

The question of how genetic variation is maintained, despite the effects of selection and drift, continues to be central to the study of evolutionary biology (Walsh & Lynch, 2018). Classical explanations include overdominance (heterozygote advantage) or frequency-dependent selection, but in the modern era of genomic data, all patterns of variation that exceed the expected variation under neutrality tend to be categorized broadly as balancing selection, regardless of the evolutionary mechanism (Mitchell-Olds *et al.*, 2007). One of the evolutionary mechanisms coined under balancing selection is sexually antagonistic selection, which occurs when the direction of natural selection on traits or loci differs between the sexes (Arnqvist & Rowe, 2013).

Sexually antagonistic selection has been identified as a powerful engine of speciation that in some cases can maintain polymorphisms in a population (Gavrilets, 2014). This sexual conflict can result in phenotypically distinct sexes that express morphological, physiological, and behavioral traits to different degrees (Mori *et al.*, 2017; Connallon & Hall, 2018). However, sexually antagonistic selection can only maintain polymorphism in specific scenarios, as classical predictions show that sexual antagonism often results in the fixation of one of the alleles (Connallon *et al.*, 2018). Importantly, the effect of sexually antagonistic selection, has been generally studied under strong simplifying assumptions such as constant population sizes and homogeneous environments (e.g., Kidwell *et al.* (1977); Pamilo (1979); Immler *et al.* (2012)). Few studies have explored the effect of sexually antagonistic selection on the maintenance of polymorphism with more realistic

assumptions. Exceptions include Connallon *et al.* (2018) who found that classical predictions break down when fluctuations in the environment combined with life-history traits allow local adaptations and promote the maintenance of genetic diversity. The effect of environmental fluctuations without local adaptation, however, has not been studied in the context of sexually antagonistic selection to the best of our knowledge.

The contribution of environmental fluctuations to genetic variability remains a debated issue in evolutionary biology. Classic theoretical models predict that temporal fluctuations in environmental conditions are unlikely to maintain a genetic polymorphism (Hedrick, 1974; 1986). However, other studies have found that fluctuating selection can maintain genetic variance on sex-linked traits (Reinhold, 2000), or in populations where generations overlap (Ellner & Hairston Jr, 1994; Ellner & Sasaki, 1996). Similarly, temporal changes in population sizes have been shown to mitigate the effect of genetic drift in small populations (Pemberton *et al.*, 1996), and in annual plant systems (Nunney, 2002). Thus, both fluctuations in selection and population sizes could dramatically change the effect of sexually antagonistic selection in the maintenance of genetic diversity.

Importantly, progress requires more than just identifying if environmental fluctuations can maintain genetic diversity in a population, but to quantify how exactly they contribute to its maintenance (Ellner *et al.*, 2016). Modern coexistence theory (MCT) provides a powerful conceptual framework to do so (Chesson, 2000b; 1994; Barabás *et al.*, 2018). Although its core ideas were formalized in an ecological context (Chesson, 1994; 2000a), this framework provides the necessary tools to examine the relative contributions of fluctuations to diversity maintenance, which can also be applied to evolutionary con-

texts (Ellner & Sasaki, 1996; Reinhold, 2000). From an ecological perspective, polymorphism of sexually antagonistic alleles is equivalent to the coexistence of species, and the fixation of either one of the alleles in a population is equivalent to competitive exclusion. The coexistence of alleles, thus, can be examined through the same lens as the coexistence of competing species.

Here, we seek to explicitly apply recent advances in MCT to the question of how polymorphism is maintained under sexually antagonistic selection. We examined how fluctuations in selection values, fluctuations in population sizes, and their interactions can stabilize or hinder the coexistence of alleles. In particular, we examined i) Can fluctuations in population sizes and selection values allow sexually antagonistic alleles to coexist when differences in their fitness would typically not allow them to? and ii) What is the relative contribution of different types of fluctuations that allow two sexually antagonistic alleles to be maintained in a population? Our study provides the tools to analyze evolutionary dynamics from a novel perspective and contributes to answering long-lasting questions regarding the effect of non-constant environments on genetic diversity.

2 Methods

We first present a model that describes the evolutionary dynamics of sexually antagonistic alleles and show how changes in allele frequencies can be expressed in terms of growth rates, a necessary condition for analyses done using modern coexistence theory. We continue by simulating different scenarios of alleles invading a population, where we allowed population sizes, selection values, both, or neither to vary. Finally, we examine

the results of our simulations through a MCT lens by calculating the contribution of each of these fluctuations in the coexistence of alleles.

Population dynamics of sexually antagonistic alleles

Our model considered evolution at single, biallelic locus with frequency and density independent effects on the relative fitness of females and males. We examined the dynamics of two sexually antagonistic alleles, j and k , that affect fitness in the haploid state. We assumed allele j always has a high fitness in females ($w_{jf} = 1$), but variable fitness in males ($w_{jm} < 1$); and allele k has a high fitness in males ($w_{km} = 1$), but variable fitness in females ($w_{kf} < 1$). The selection against allele j in males is therefore $S_m = 1 - w_{jm}$, and the selection against allele k in females is $S_f = 1 - w_{kf}$.

The frequency of each allele in each sex at the beginning of a life-cycle at time t is given by:

$$p_{jm,t} = \frac{n_{jm,t}}{N_{m,t}} \quad (1)$$

$$p_{jf,t} = \frac{n_{jf,t}}{N_{f,t}} \quad (2)$$

$$p_{km,t} = \frac{N_{m,t} - n_{jm,t}}{N_{m,t}} \quad (3)$$

$$p_{kf,t} = \frac{N_{f,t} - n_{jf,t}}{N_{f,t}} \quad (4)$$

where $N_{m,t}$ and $N_{f,t}$ are the numbers of males and females in a population at time t , $n_{jf,t}$ is the number of females f with allele j , and $n_{jm,t}$ is the number of males m with allele j at time t , respectively.

91 The individuals in the population mate at random before selection occurs, and there-
 92 fore the frequency of offspring with allele j after mating, $p'_{j,t}$ can be expressed as:

$$p'_{j,t} = \frac{n_{jf}}{N_f} \frac{n_{jm}}{N_m} + \frac{1}{2} \frac{n_{jf}}{N_f} \frac{(N_m - n_{jm})}{N_m} + \frac{1}{2} \frac{(N_f - n_{jf})}{N_f} \frac{n_{jm}}{N_m}, \quad (5)$$

93 which upon rearranging and simplifying gives:

$$p'_{j,t} = \frac{(N_{m,t}n_{jf,t} + N_{f,t}n_{jm,t})}{2N_fN_m}. \quad (6)$$

94 Selection acts upon these offspring in order to determine the allelic frequencies in females
 95 and males in the next generation, $t + 1$. As an example the frequency of females with
 96 allele j after selection is given by:

$$p'_{jf,t+1} = \frac{n_{jf,t+1}}{N'_{f,t+1}} = \frac{p'_j w_{jf}}{p'_j w_{jf} + (1 - p'_j) w_{kf}} \quad (7)$$

97 The logarithmic growth rate of j in females, is therefore given by the number of fe-
 98 males with allele j after selection, divided by the original number of females carrying
 99 allele j :

$$r_{jf,t} = \ln \left(\frac{n'_{jf,t+1}}{n_{jf,t}} \right) \quad (8)$$

100 An equivalent expression for the per capita growth rate of allele j in males m can be
 101 obtained by exchanging f for m across the various subscripts in this expression.

102 Allelic coexistence in a sexual population, however, is ultimately influenced by growth

and establishment of an allele across both sexes. Therefore, the full growth rate of allele j across the entire population of females *and* males is given by:

$$r_j = \ln \left(\frac{n'_{jf,t+1} + n'_{jm,t+1}}{n_{jf,t} + n_{jm,t}} \right) . \quad (9)$$

An equivalent expression describes r_k , the growth rate of allele k .

Selection maintains both alleles in the population under the condition that:

$$\frac{S_m}{1 + S_m} < S_f < \frac{S_m}{1 - S_m} \quad (10)$$

(Kidwell *et al.*, 1977; Pamilo, 1979; Connallon & Hall, 2018) Thus, the maintenance of polymorphism of sexually antagonistic alleles is solely determined by the values of S_m and S_f . Note that in our model, the values S_m and S_f are bounded from 0 to 1. Therefore the **parameter space of sexually antagonistic selection** is within the range $0 < S_m, S_f < 1$. Classic theoretical models predict that in constant environments, only in ≈ 0.38 of the selection parameter space alleles can coexist (Kidwell *et al.*, 1977; Pamilo, 1979; Connallon *et al.*, 2018). If fluctuations in population sizes or selection values have an effect on the coexistence of sexually antagonistic alleles, it would be reflected in increases or decreases of the proportion of the parameter space of selection where polymorphism is maintained.

Simulations

Typically, MCT would require decomposing alleles' growth rates (e.g., Eqn. 9) analytically to examine the relative contributions of different types of fluctuations to their coexistence

(Barabás *et al.*, 2018). Although we present an analytical approach in the Supporting Information, our general solution is not easily interpretable and soon becomes mathematically intractable (S1 Supporting Information). Thus, we opted for an extension of MCT that provides the flexibility to examine the contributions of different processes to coexistence using simulations (Ellner *et al.*, 2019; Shoemaker *et al.*, 2020).

For each simulation, we examined coexistence outcomes across the selection parameter space of sexually antagonistic selection ($0 < S_m, S_f < 1$). To do so, we partitioned the parameter space into a grid of 50×50 , which yielded 2500 pairwise combinations of different w_{jm} and w_{kf} values. For each pairwise combination of w_{jm} and w_{kf} , as we detail in the next sections, we iterated our model while controlling the effect size of fluctuations in selection (σ_w) and their correlation (ρ_w), as well as fluctuations in population sizes (σ_g) and their correlation (ρ_g). Then, we performed “invasion simulations” of each allele invading a population, evaluated coexistence outcomes, and determined the relative contribution of each type of fluctuation. Finally, we calculated for each simulation the proportion of the parameter space that allowed alleles to coexist.

We explored all of the combinations of low, intermediate, and high fluctuations in fitness values and population sizes, with different extents of correlations between fluctuations (Table 1). As a control simulation, we set $\sigma_w = 0.001$ and $\sigma_g = 0.001$, with no correlation between fluctuations. We ran ten replicates per parameter combination, which resulted in 3780 simulations.

139 Timeseries

140 To incorporate the effects of fluctuations into our population dynamics model we gener-
 141 ated independent timeseries of fluctuations in selection and population sizes. In the case
 142 of fluctuations in selection values, for a given value of w_{jm} and w_{kf} (i.e., a fixed point
 143 in the selection parameter space), we generated a timeseries of 500 timesteps made up
 144 of correlated fluctuations of w_{jm} and w_{kf} . We controlled the effect size of fluctuations in
 145 selection (σ_w) and its correlation (ρ_w) by using the Cholesky factorization of the variance-
 146 covariance matrix:

$$C_w = \begin{bmatrix} \sigma_w^2 & \rho_w \sigma_w^2 \\ \rho_w \sigma_w^2 & \sigma_w^2 \end{bmatrix} \quad (11)$$

147 We multiplied Eqn. 11 by a (2×500) matrix of random numbers from a normal distri-
 148 bution with mean 0 and unit variance, which yielded γ_j and γ_k . Then, we calculated the
 149 new fitness values at time $t + 1$ as $w_{jm,t+1} = w_{jm}^{\gamma_{j,t}}$ and $w_{kf,t+1} = w_{kf}^{\gamma_{k,t}}$.

150 Similarly, we generated a timeseries of 500 timesteps made up of correlated fluctu-
 151 ations in population sizes. We chose values of $N_m = 200$ and $N_f = 200$ as the initial
 152 value of population sizes throughout our simulations. We performed a Cholesky fac-
 153 torization of the variance-covariance matrix, controlling the effect size of fluctuations in
 154 population sizes with σ_g and their correlation with ρ_g . Similar to our previous approach,
 155 we multiplied this factorization by a random matrix of uncorrelated random variables,
 156 which yielded γ_m and γ_f . Finally, we calculated the number of males and females in the
 157 population at time $t + 1$ as $N_{m,t+1} = N_m + \gamma_{m,t}$ and $N_{f,t+1} = N_f + \gamma_{f,t}$. Therefore, the

population sizes in each timestep differed from the initial value of 200 individuals on the order of ρ_g . Note that the scales of σ_g and σ_w are different from each other. While σ_w controls the exponential change in fitness values in each timestep, σ_g controls the number of individuals added to a population in each timestep.

Finally, we performed simulations where our population dynamics model (Eqns. 1 to 9) iterated over 500 timesteps while allowing selection values and population sizes to fluctuate in each timestep. We started each simulation with the initial values of N_m and N_f described before and equal frequencies of allele j and allele k in each sex. For each timestep t in our simulations, the values of w_{jm} , w_{kf} , N_m and N_f used to calculate allele's frequencies in timestep t (e.g., Eqn. 7), corresponded to the t values calculated in each timeseries, as described previously. This approach yielded a final timeseries that captured the dynamics of sexually antagonistic alleles, with fluctuating values of selection and population sizes.

Invasion simulations

Modern coexistence theory has shown that coexistence is promoted by mechanisms that give species a population growth rate advantage over other species when they become rare (Chesson, 1982; 2003; Barabás *et al.*, 2018). Typically, one species is held at its *resident* state, as given by its steady-state abundances while the rare species is called the *invader*. In the context of alleles in a population, an allele is an *invader* when a mutation occurs that introduces that allele into a population in which it is absent (e.g., if in a population with only k alleles, a random mutation made one individual carry the j al-

lele). Within sexually antagonistic selection, each allele has two pathways of invasion, depending on whether the mutation arises in a female or in a male. If an allele's *invasion growth rate* (or the average instantaneous population growth rate when rare) is positive, it buffers it against extinction, maintaining its persistence in the population. Coexistence, and hence polymorphism, occurs when both alleles have positive invasion growth rates.

We used the timeseries that captured the dynamics of our population model as a template to perform invasion simulations of both alleles. We performed 500 independent invasion simulations, one for each timestep in our timeseries. We explored all four potential combinations of each allele invading through each pathway (e.g., allele j invading through males, and allele k invading through females, and so on). To simulate invasion, we set the density of the invading allele to one individual. For example, if allele j was invading via males, then we would set $n_{jm,i} = 1$ and $n_{jf,i} = 0$. Note that each invasion simulation was independent of the iteration that we used to generate the timeseries, therefore we denoted the initial timestep in an invasion simulation with the subscript i . We also set the resident allele, in this case k , to the corresponding value of the timeseries minus one individual, $n_{km,i} = N_{m,t} - 1$ and $n_{kf,i} = N_{f,t}$. Then, we iterated our model one timestep, $i + 1$, and calculated the logarithmic growth rate of j allele invading as:

$$r_j = \ln \left(\frac{n_{jm,i+1} + n_{jf,i+1}}{1} \right) \quad (12)$$

Correspondingly, the logarithmic growth rate of the k allele as a resident would be

197 given by:

$$r_k = \ln \left(\frac{n_{km,i+1} + n_{kf,i+1}}{n_{km,i} + n_{kf,i}} \right) \quad (13)$$

198 Following the approach of Shoemaker *et al.* (2020), we treated each invasion simula-
199 tion independently, and hence we performed 500 invasion simulations. We then calcu-
200 lated, for each allele invading via a different pathway, its mean invasion growth rate as
201 the average of the 500 invasion growth rates. We also calculated the mean growth rate of
202 the resident allele as the average of the 500 resident growth rates. We determined alleles
203 to be coexisting if both of alleles had positive mean invasion growth rates, which is often
204 referred to as the mutual invasibility criterion (Barabás *et al.*, 2018).

205 **Functional decomposition**

206 Our invasion simulations tell us whether or not sexually antagonistic alleles can coex-
207 ist in a determined point of the selection parameter space. However, we also quantified
208 the relative contributions of fluctuating selection and population sizes into the predicted
209 coexistence outcome using a *functional decomposition* approach (Ellner *et al.*, 2016; 2019;
210 Shoemaker *et al.*, 2020).

211 We applied the functional decomposition approach by breaking up the average growth
212 rate of each allele into a null growth rate in the absences of fluctuations in all selected vari-
213 ables, a set of main effect terms that represent the effect of only one variable fluctuating,
214 and a set of two-way interaction terms representing the effect of variables fluctuating si-
215 multaneously (Ellner *et al.*, 2019). In our simulations, this is a function of four variables:
216 the number of males in the population (N_m), the number of females in the population

217 (N_f), the fitness of allele j in males (w_{jm}), and the fitness of allele k in females (w_{kf}). As
 218 an example, if only N_m and N_f were fluctuating, the growth rate of allele j when it is the
 219 invader at timestep t could be decomposed into:

$$r_{j,t}(N_m, N_f) = \mathcal{E}_j^0 + \mathcal{E}_j^{N_m} + \mathcal{E}_j^{N_f} + \mathcal{E}_j^{N_m N_f} \quad (14)$$

220 Where \mathcal{E}^0 is the null growth rate when N_m and N_f are set to their averages. Terms
 221 with superscripts represent the marginal effects of letting all superscripted variables vary
 222 while fixing all the other variables at their average values. For example, the term \mathcal{E}^{N_m}
 223 expresses the contribution of fluctuations in N_m when N_f is at its average, without the
 224 contribution when both variables are set to their averages :

$$\mathcal{E}_j^{N_m} = r_{j,t}(N_m, \overline{N_f}) - \mathcal{E}_j^0 \quad (15)$$

225 If we average Eqn. 14 across the timesteps in our simulation, we get a partition of
 226 the average population growth rate into the variance-free growth rate, the main effects
 227 of variability in N_m , the main effects of variability in N_f , and the interaction between
 228 variability in N_m and N_f

$$\bar{r}_j = \mathcal{E}_j^0 + \overline{\mathcal{E}_j^{N_m}} + \overline{\mathcal{E}_j^{N_f}} + \overline{\mathcal{E}_j^{N_m N_f}} \quad (16)$$

229 However, in our simulations w_{jm} and w_{kf} also fluctuated, therefore the full functional
 230 decomposition of the growth rate of allele j as an invader is found in Table 2, as well as
 231 a brief description of the meaning of each term. The implementation and interpretation

232 of the functional decomposition of the invasion growth rates of each allele are identical
 233 to each other. Note that Table 2 does not include three or four-way interactions (e.g.,
 234 $\bar{\mathcal{E}}_j^{N_m N_f w_{jm} w_{fk}}$). This is because in our simulations, we did not allow fluctuations in selection
 235 and population sizes to be correlated, therefore their effects are solely captured by the
 236 terms in Table 2. We calculated the value of each of the terms in Table 2 by performing
 237 another set of invasion simulations as described previously, but instead of allowing all
 238 variables to fluctuate, systematically setting the required variables to their means and
 239 subtracting the corresponding \mathcal{E} values.

240 The functional decomposition approach further requires the *comparison* of each term,
 241 to understand if how it affects invaders and residents. This is because fluctuations can
 242 promote coexistence by helping whichever allele is rare, or they can hurt whichever allele
 243 is common. Therefore, to understand the role of each type of fluctuation, it is necessary
 244 to compare how it affects invader *and* resident growth rates. In the example presented
 245 in Eqn. 16, if allele j is invading, then allele k is at its resident state and there exists an
 246 analogue decomposition of \bar{r}_k with the exact same terms as Eqn. 16. Therefore we can
 247 express the difference between contributions of fluctuations in N_m as:

$$\Delta_j^{N_m} = \bar{\mathcal{E}}_j^{N_m} - \bar{\mathcal{E}}_k^{N_m} \quad (17)$$

248 If $\Delta_j^{N_m}$ is positive, then fluctuations in the male population benefit allele j when it is
 249 rare more than what they benefit k as a resident. If $\Delta_j^{N_m}$ is negative, then fluctuations
 250 benefit k as a resident more than j as an invader, and if it is minimal, then fluctuations

have an equal effect in j and k . Therefore, for each allele invading via a different pathway, we calculated 11 Δ values, one for each one of the \mathcal{E} terms in Table 2. However, since the magnitude of each one of these values could vary considerably across the parameter space of selection, to make them comparable, we normalized each Δ value by dividing it by the square root of the sum of the squares of the 11 Δ values. For example, the normalized value of Eqn. 17 would be given by:

$$\delta_j^{N_m} = \frac{\Delta_j^{N_m}}{\sqrt{\sum_{d=1}^{11} (\Delta_d)^2}} \quad (18)$$

This normalization bounded δ values from -1 to 1 .

3 Results

Our results showed that both fluctuations in selection and in population sizes can substantially increase the expected genetic variability under sexually antagonistic selection. The average proportion of coexistence in the selection parameter space increased with the effect size of fluctuations when fluctuations were large enough (Fig. 1). Fluctuations with small effect sizes either decreased or matched the average proportion of the parameter space of allelic coexistence compared to the control simulation (Fig. 1). Increments in allelic coexistence were more likely when fluctuations were large, and fluctuations in population sizes were negatively correlated, while fluctuations in selection were positively correlated (Fig. 1).

Fluctuations increased coexistence by allowing both alleles to have a positive inva-

sion growth rate in instances where selection would typically not allow them to (i.e., they made parts of the parameter space “flip” into coexistence). As a baseline, we show in Fig. 2A the outcome of the control simulation, which matches previous findings that without fluctuations, alleles can coexist in only ≈ 0.38 of the selection parameter space (Connallon & Hall, 2018). These “flips” occurred with both types of fluctuations and were more common with larger fluctuations and strongly correlated effects, for which we show examples in Fig. 2A . However, note that there are also parts of the parameter space where coexistence is lost compared to the control simulation, which was more likely when population sizes were fluctuating (Fig. 2A).

Alleles had positive invasion growth rates when positive contributions of fluctuations outweighed the negative contributions of fluctuations. As an example in Fig. 2B we show the functional decomposition of both alleles invading via their favoured pathway in parts of the parameter space that “flipped” into coexistence and competitive exclusion (which correspond to the square and triangle in Fig. 2A). Note that each type of fluctuation made similar contributions to each allele, both when they were coexisting or experiencing competitive exclusion (Fig. 2B). However, δ_0 , which captures the effect of fluctuations set to their averages, captured both positive and negative contributions for both alleles (Fig. 2B).

The relative contribution of fluctuations in population sizes depended on the sex where invasion occurred (Fig. 2B and Fig. 3).

Figures and tables

Table 1: Parameters used in our simulations to control the effect size of fluctuations in population sizes (σ_g) and selection values (σ_w), as well as their respective correlations (ρ_g and ρ_w). We ran ten replicates for each one of the factorial combinations of the following parameters.

Parameter	Values	Description
σ_w	0.001, 0.1, 0.3, 0.5, 0.7, 0.9	Effect size of fluctuations in fitness values
σ_g	0.001, 1, 10, 20, 30, 50	Effect size of fluctuations in population sizes
ρ_w	-0.75, 0, 0.75	Correlation between fluctuations in fitness values
ρ_g	-0.75, 0, 0.75	Correlation between fluctuation in population sizes

Table 2: Functional decomposition of the growth rate of allele j . As we show in Eqn. 16, each term captures the contribution of fluctuations to an alleles' invasion growth rate.

Term	Formula	Meaning
\mathcal{E}_j^0	$\bar{r}_j(\bar{N}_m, \bar{N}_f, \bar{w}_{jm}, \bar{w}_{kf})$	Growth rate at mean population size and fitness values.
$\bar{\mathcal{E}}_j^{N_m}$	$\bar{r}_j(N_m, \bar{N}_f, \bar{w}_{jm}, \bar{w}_{kf}) - \mathcal{E}_j^0$	Main effect of fluctuations in N_m
$\bar{\mathcal{E}}_j^{N_f}$	$\bar{r}_j(\bar{N}_m, N_f, \bar{w}_{jm}, \bar{w}_{kf}) - \mathcal{E}_j^0$	Main effect of fluctuations in N_f
$\bar{\mathcal{E}}_j^{w_{jm}}$	$\bar{r}_j(\bar{N}_m, \bar{N}_f, w_{jm}, \bar{w}_{kf}) - \mathcal{E}_j^0$	Main effect of fluctuations in w_{jm}
$\bar{\mathcal{E}}_j^{w_{kf}}$	$\bar{r}_j(\bar{N}_m, \bar{N}_f, \bar{w}_{jm}, w_{kf}) - \mathcal{E}_j^0$	Main effect of fluctuations in w_{kf}
$\bar{\mathcal{E}}_j^{N_m, N_f}$	$\bar{r}_j(N_m, N_f, \bar{w}_{jm}, \bar{w}_{kf}) - [\mathcal{E}_j^0 + \bar{\mathcal{E}}_j^{N_m} + \bar{\mathcal{E}}_j^{N_f}]$	Interaction of fluctuations in N_m and N_f
$\bar{\mathcal{E}}_j^{w_{jm}, w_{kf}}$	$\bar{r}_j(\bar{N}_m, \bar{N}_f, w_{jm}, w_{kf}) - [\mathcal{E}_j^0 + \bar{\mathcal{E}}_j^{w_{jm}} + \bar{\mathcal{E}}_j^{w_{kf}}]$	Interaction of fluctuations in w_{jm} and w_{kf}
$\bar{\mathcal{E}}_j^{N_m, w_{jm}}$	$\bar{r}_j(N_m, \bar{N}_f, w_{jm}, \bar{w}_{kf}) - [\mathcal{E}_j^0 + \bar{\mathcal{E}}_j^{N_m} + \bar{\mathcal{E}}_j^{w_{jm}}]$	Interaction of fluctuations in N_m and w_{jm}
$\bar{\mathcal{E}}_j^{N_m, w_{kf}}$	$\bar{r}_j(N_m, \bar{N}_f, \bar{w}_{jm}, w_{kf}) - [\mathcal{E}_j^0 + \bar{\mathcal{E}}_j^{N_m} + \bar{\mathcal{E}}_j^{w_{kf}}]$	Interaction of fluctuations in N_m and w_{kf}
$\bar{\mathcal{E}}_j^{N_f, w_{jm}}$	$\bar{r}_j(\bar{N}_m, N_f, w_{jm}, \bar{w}_{kf}) - [\mathcal{E}_j^0 + \bar{\mathcal{E}}_j^{N_f} + \bar{\mathcal{E}}_j^{w_{jm}}]$	Interaction of variation in N_f and w_{jm}
$\bar{\mathcal{E}}_j^{N_f, w_{kf}}$	$\bar{r}_j(\bar{N}_m, N_f, \bar{w}_{jm}, w_{kf}) - [\mathcal{E}_j^0 + \bar{\mathcal{E}}_j^{N_f} + \bar{\mathcal{E}}_j^{w_{kf}}]$	Interaction of fluctuations N_f and w_{kf}

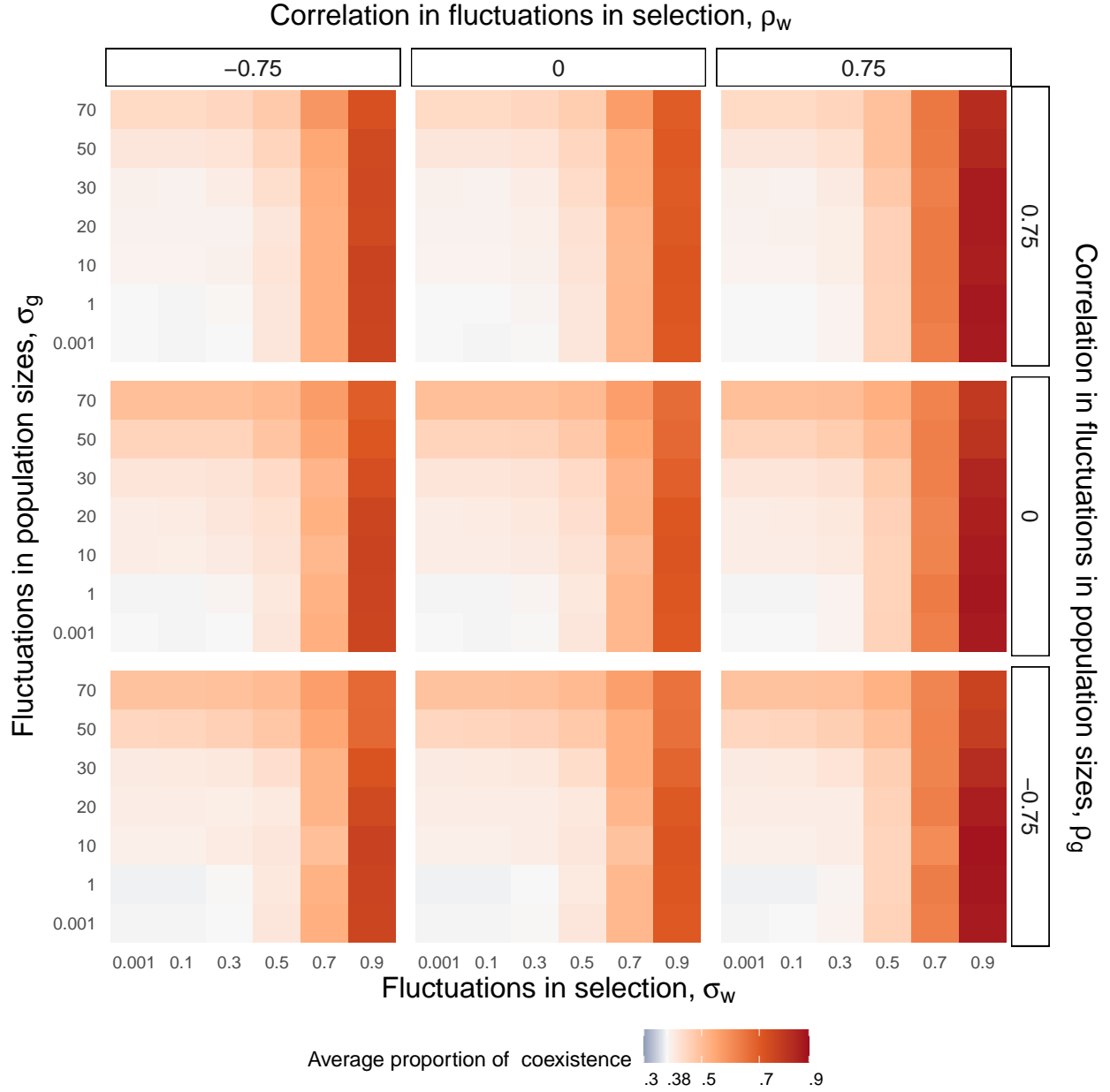


Figure 1: Average proportion of coexistence for different parameter combinations. We show, for all factorial combinations of values of σ_g , σ_w , ρ_g and ρ_w , the average proportion of coexistence of in our simulations. Each panel corresponds to a different combination of correlations between fluctuations. Labels on top indicate the correlation between fluctuations in selection ρ_w , while labels on the right show the correlation in fluctuations between fluctuations in population sizes ρ_g . As a basis of comparison, we show the expected proportion of coexistence (0.38) as the midpoint in our color scheme.

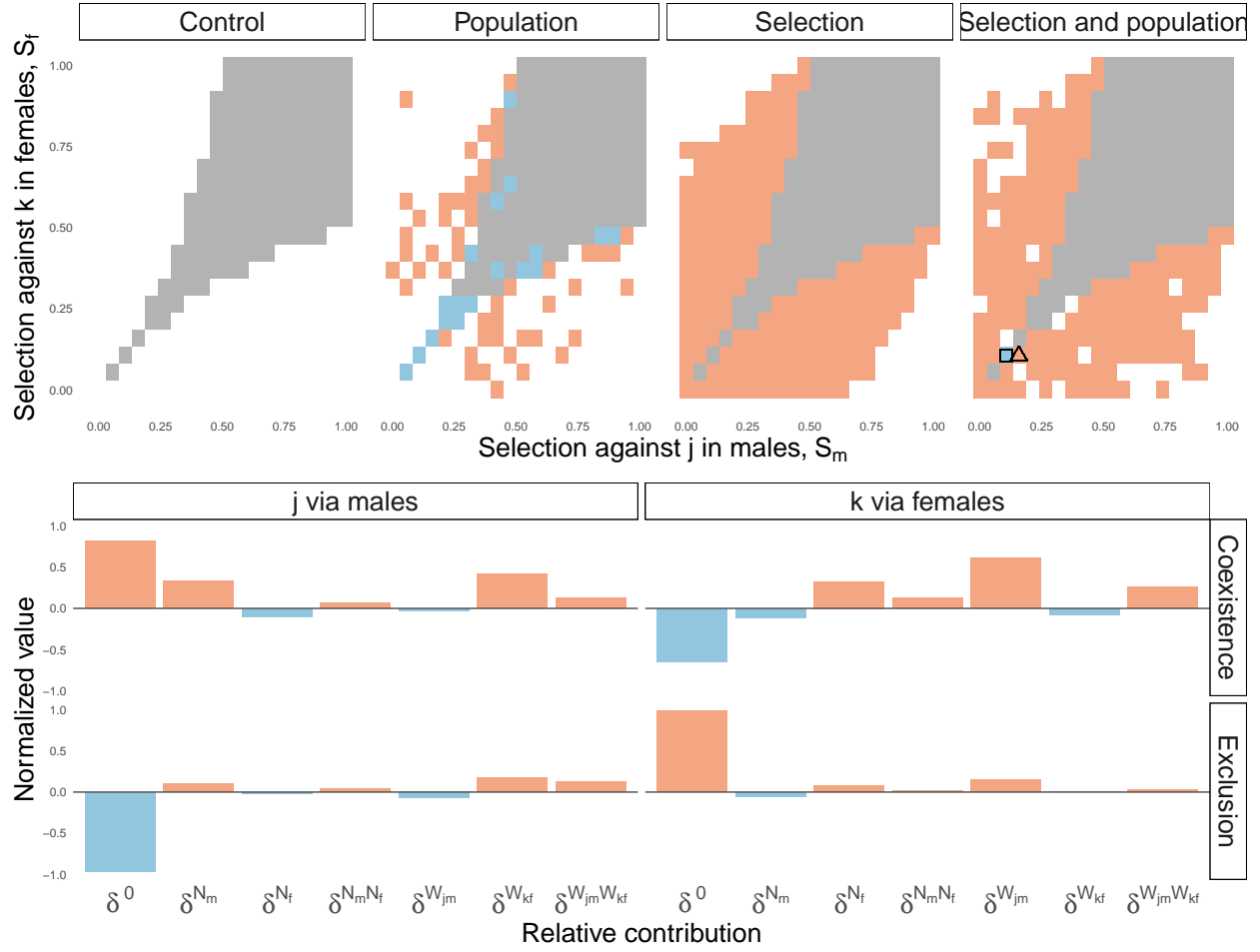


Figure 2: Coexistence outcomes and functional decomposition of one simulation. We show in A) for one of the replicates highlighted with a white square in Fig. ?? ($\sigma_g = 70$, $\sigma_w = 0.9$, $\rho_g = -0.75$ and $\rho_{w=0.75}$) the coexistence outcomes when j invades via females and k invades via males. Grey areas denote points in the parameter space where alleles can coexist, while white areas are points where at least one allele does not have a positive invasion growth rate. We highlight in black a point in the parameter space where coexistence is lost compared to the control simulation. In B) we show for the same simulation, the functional decomposition of each allele across the parameter space of selection. The highlighted black points correspond to the same point shown in A).

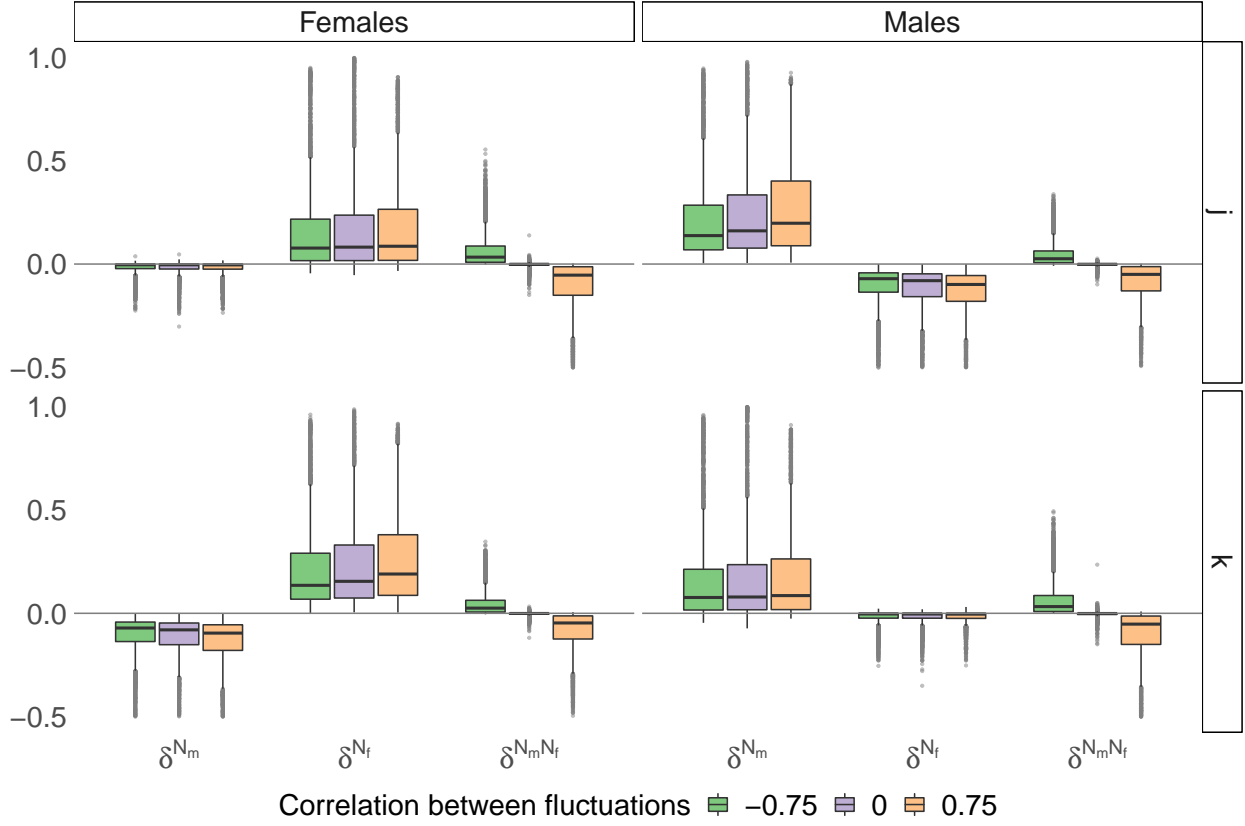


Figure 3: Boxplots of δ values. In A) we show the box plots of δ values that capture the relative contributions of fluctuations in population sizes, for all of the replicates in our simulation in which $\sigma_g = 70$ and $\sigma_w = 0.001$. Labels on top indicate the correlation between fluctuations in population sizes, ρ_g . Each color corresponds to a different allele and invasion pathway in our simulations. In B) we show the box plots of δ values that capture the contributions of fluctuations in selection, for all of the replicates in our simulation in which $\sigma_w = 0.9$ and $\sigma_g = 0.001$. Labels on top indicate the correlation between fluctuations in selection, ρ_w , with the same color nomenclature as in A). Each box plot extends from the first to third quantiles of the corresponding posterior distribution of parameter values, and the line inside the box indicates the median. The upper whisker extends to the largest value no further than 1.5 times the inter-quantile range (IQR, or the distance between the first and third quantiles); the lower whisker extends to the smallest value at most 1.5 times the IQR. Data beyond the end of the whiskers are determined to be outliers and are plotted individually with solid grey points.

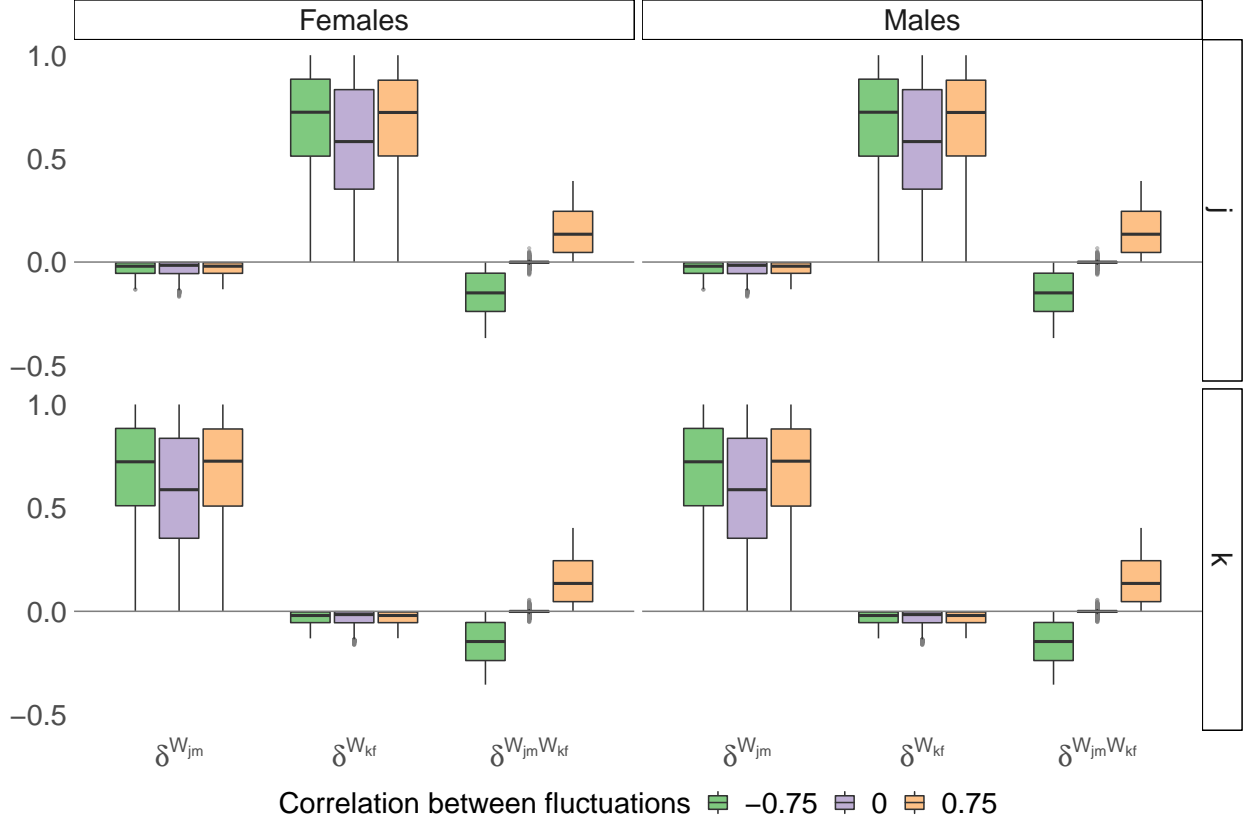


Figure 4: Boxplots of δ values. In A) we show the box plots of δ values that capture the relative contributions of fluctuations in population sizes, for all of the replicates in our simulation in which $\sigma_g = 70$ and $\sigma_w = 0.001$. Labels on top indicate the correlation between fluctuations in population sizes, ρ_g . Each color corresponds to a different allele and invasion pathway in our simulations. In B) we show the box plots of δ values that capture the contributions of fluctuations in selection, for all of the replicates in our simulation in which $\sigma_w = 0.9$ and $\sigma_g = 0.001$. Labels on top indicate the correlation between fluctuations in selection, ρ_w , with the same color nomenclature as in A). Each box plot extends from the first to third quantiles of the corresponding posterior distribution of parameter values, and the line inside the box indicates the median. The upper whisker extends to the largest value no further than 1.5 times the inter-quantile range (IQR, or the distance between the first and third quantiles); the lower whisker extends to the smallest value at most 1.5 times the IQR. Data beyond the end of the whiskers are determined to be outliers and are plotted individually with solid grey points.

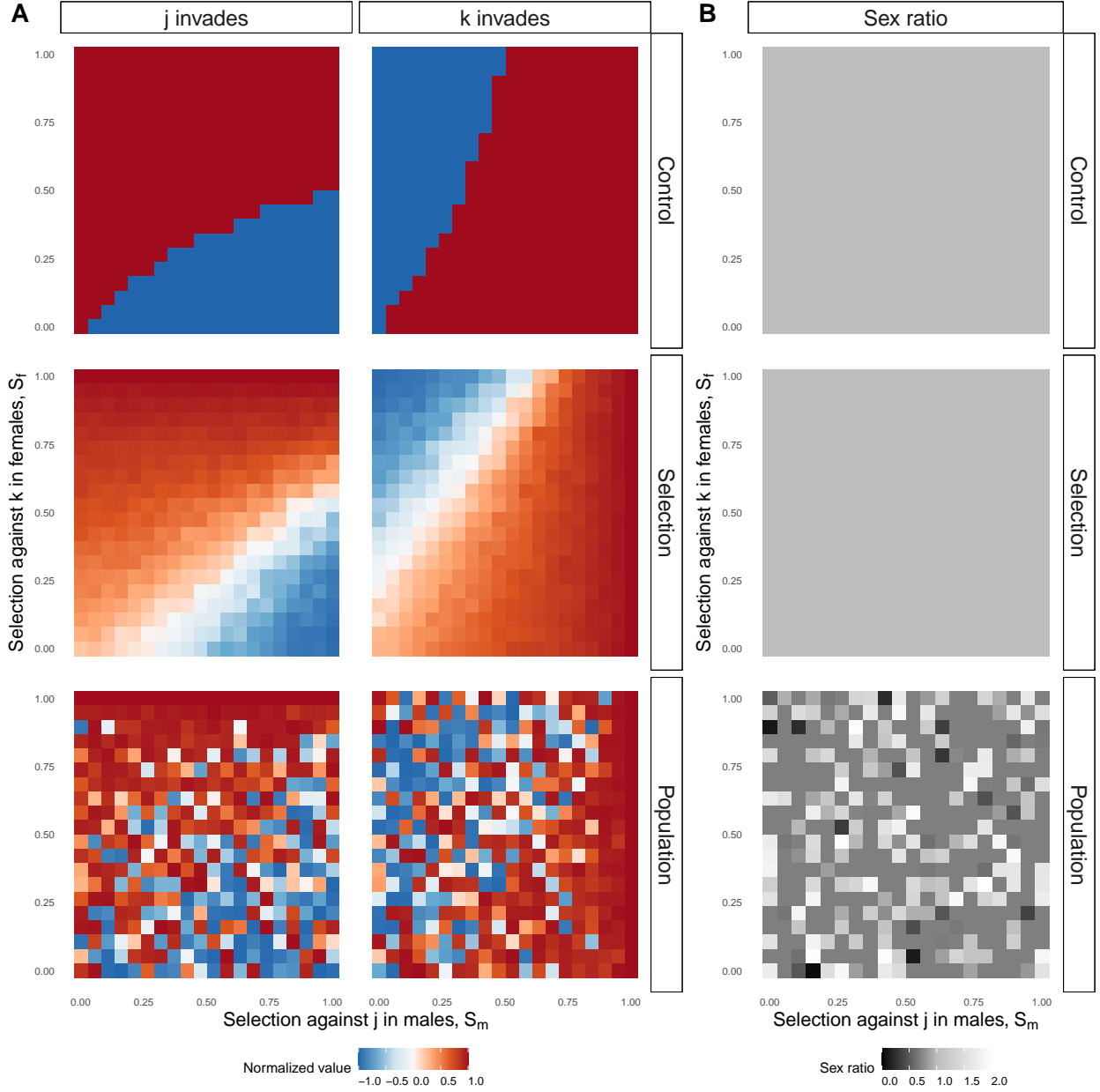


Figure 5: The relationship between δ^0 and sex ratios. In A) we show the values of δ^0 across the selection parameter space for different types of simulations when j invades via males and k invades via females. Each pannel corresponds to an allele invading a population in a replicate of different simulations, as labels on the right indicate: Control denotes the control simulation, Selection denotes a simulation where $\sigma_w = 0.9$ and $\sigma_g = 0.001$, and Population indicates a simulation where $\sigma_w = 0.001$ and $\sigma_g = 70$. For simplicity we kept both correlations equal to zero. In B), we show for the same replicates shown in A), the sex ratios, calculated as $\frac{N_f}{N_m}$, across the selection parameter space.

References

- Arnqvist, G. & Rowe, L. (2013). *Sexual conflict*. Princeton University Press.
- Barabás, G., D'Andrea, R. & Stump, S.M. (2018). Chesson's coexistence theory. *Ecological Monographs*, 88, 277–303.
- Chesson, P. (1994). Multispecies competition in variable environments. *Theoretical population biology*, 45, 227–276.
- Chesson, P. (2000a). General theory of competitive coexistence in spatially-varying environments. *Theoretical Population Biology*, 58, 211–237.
- Chesson, P. (2000b). Mechanisms of maintenance of species diversity. *Annual review of Ecology and Systematics*, 31, 343–366.
- Chesson, P. (2003). Quantifying and testing coexistence mechanisms arising from recruitment fluctuations. *Theoretical Population Biology*, 64, 345–357.
- Chesson, P.L. (1982). The stabilizing effect of a random environment. *Journal of Mathematical Biology*, 15, 1–36.
- Connallon, T. & Hall, M.D. (2018). Environmental changes and sexually antagonistic selection. *eLS*, pp. 1–7.
- Connallon, T., Sharma, S. & Olito, C. (2018). Evolutionary Consequences of Sex-Specific Selection in Variable Environments: Four Simple Models Reveal Diverse Evolutionary Outcomes. *The American Naturalist*, 193, 93–105.

- Ellner, S. & Hairston Jr, N.G. (1994). Role of overlapping generations in maintaining genetic variation in a fluctuating environment. *The American Naturalist*, 143, 403–417.
- Ellner, S. & Sasaki, A. (1996). Patterns of genetic polymorphism maintained by fluctuating selection with overlapping generations. *theoretical population biology*, 50, 31–65.
- Ellner, S.P., Snyder, R.E. & Adler, P.B. (2016). How to quantify the temporal storage effect using simulations instead of math. *Ecology letters*, 19, 1333–1342.
- Ellner, S.P., Snyder, R.E., Adler, P.B. & Hooker, G. (2019). An expanded modern coexistence theory for empirical applications. *Ecology Letters*, 22, 3–18.
- Gavrilets, S. (2014). Is sexual conflict an “engine of speciation”? *Cold Spring Harbor perspectives in biology*, 6, a017723.
- Hedrick, P.W. (1974). Genetic variation in a heterogeneous environment. i. temporal heterogeneity and the absolute dominance model. *Genetics*, 78, 757–770.
- Hedrick, P.W. (1986). Genetic polymorphism in heterogeneous environments: a decade later. *Annual review of ecology and systematics*, 17, 535–566.
- Immler, S., Arnqvist, G. & Otto, S.P. (2012). Ploidally antagonistic selection maintains stable genetic polymorphism. *Evolution: International Journal of Organic Evolution*, 66, 55–65.
- Kidwell, J., Clegg, M., Stewart, F. & Prout, T. (1977). Regions of stable equilibria for models of differential selection in the two sexes under random mating. *Genetics*, 85, 171–183.

- Mitchell-Olds, T., Willis, J.H. & Goldstein, D.B. (2007). Which evolutionary processes influence natural genetic variation for phenotypic traits? *Nature Reviews Genetics*, 8, 845–856.
- Mori, E., Mazza, G. & Lovari, S. (2017). Sexual dimorphism. *Encyclopedia of Animal Cognition and Behavior* (J. Vonk, and T. Shakelford, Eds). Springer International Publishing, Switzerland, pp. 1–7.
- Nunney, L. (2002). The effective size of annual plant populations: the interaction of a seed bank with fluctuating population size in maintaining genetic variation. *The American Naturalist*, 160, 195–204.
- Pamilo, P. (1979). Genic variation at sex-linked loci: Quantification of regular selection models. *Hereditas*, 91, 129–133.
- Pemberton, J., Smith, J., Coulson, T.N., Marshall, T.C., Slate, J., Paterson, S., Albon, S., Clutton-Brock, T.H. & Sneath, P.H.A. (1996). The maintenance of genetic polymorphism in small island populations: large mammals in the hebrides. *Philosophical Transactions of the Royal Society of London. Series B: Biological Sciences*, 351, 745–752.
- Reinhold, K. (2000). Maintenance of a genetic polymorphism by fluctuating selection on sex-limited traits. *Journal of Evolutionary Biology*, 13, 1009–1014.
- Shoemaker, L.G., Barner, A.K., Bittleston, L.S. & Teufel, A.I. (2020). Quantifying the relative importance of variation in predation and the environment for species coexistence. *Ecology letters*, 23, 939–950.

³⁴⁹ Walsh, B. & Lynch, M. (2018). *Evolution and Selection of Quantitative Traits*. OUP Oxford.